Available online at www.sciencedirect.com
ScienceDirect
Journal of the European Ceramic Society 30 (2010) 713–725
www.elsevier.com/locate/jeurceramsoc

Fatigue failure characteristics of lead zirconate titanate piezoelectric ceramics

Mitsuhiro Okayasu *, Go Ozeki, Mamoru Mizuno

Department of Machine Intelligence and Systems Engineering, Akita Prefectural University, 84-4 Ebinokuchi, Tuchiya-aza, Yurihonjo-city, Akita, 015-0055, Japan

Received 17 April 2009; received in revised form 30 August 2009; accepted 11 September 2009
Available online 6 October 2009

Abstract

Mechanical properties and fatigue failure characteristics of lead zirconate titanate piezoelectric ceramic (PZT) have been investigated. Bending and fatigue strengths of PZT ceramic are directly attributed to the electrode status. Material hardening occurs in the PZT ceramic during the cyclic loading, which is influenced by domain switching occurring anywhere in the grains. The domain structure is clearly detected by electron back scatter diffraction analysis and etching techniques. It also appears that the poling direction causes the change of failure characteristics due to different domain and domain wall orientation. The domain orientation changes alternately from domain to domain by 90°. Moreover, the domain wall orientation is well regulated in the grains perpendicular to the poling direction. An acceleration of fatigue crack growth occurs as the crack propagates along the domain wall.

Keywords: PZT; Piezoelectric properties; Domain switching; Fatigue; Fracture

1. Introduction

The lead zirconate titanate (PZT) ceramics have been subjected to intensive research world-wide since the ceramic was developed in the middle of the twentieth century. The piezoelectric ceramic offers promising electrical applications in many smart structures, and PZT is regularly employed in a number of actuators and sensors. As the size of the actuator becomes smaller and the need for structural integrity and reliability increases, ceramics with good mechanical properties are needed.[1] The durability of ceramics in various conditions is also important to allow applications over a long period of time.[2] Because PZT ceramics in smart structures demands high material performance, an examination of the material response to the application is significant. The efficiency of the piezoelectric may change when the operational time increases, due to the change of material properties. There are various PZT ceramics with different (i) material characteristics (soft and hard); (ii) electrode materials (silver and nickel) and (iii) poling direction. In the study by Guillon et al., the fracture characteristics of soft and hard PZTs were examined.[3] From their work, differences in the fracture mechanism between hard and soft ceramics were clarified. The Weibull parameters in hard PZT were found to be higher than those for soft ones. In addition, it appeared that the crack propagates mainly through the grain in the hard sample (transgranular), while it grows in the grain boundary in the soft ceramic (intergranular).[3]

A number of electrode materials have been utilized for PZT ceramics, e.g., nickel and silver. The plating materials are printed on the substrate using different processes, a firing process for a Ag electrode and electroplating for a Ni electrode. In previous work, the effect of the Ag electrode on the fatigue properties of PZT was examined since the electrode materials are understood to play an important role in the mechanical properties of PZT ceramics.[4,5] It appeared that the electrode could make a reduction in the material strength of PZT. The reasons behind this are (i) microcracks generated from a porous region[3,5] and (ii) electrogeneration trapped at a defect.[6] Even though the influence of the electrode on the fatigue properties has been investigated for Ag–PZT samples, this examination has not been carried out for

* Corresponding author.
E-mail address: okayasu@akita-pu.ac.jp (M. Okayasu).

0955-2219/$ – see front matter © 2009 Elsevier Ltd. All rights reserved.
doi:10.1016/j.jeurceramsoc.2009.09.014

Ni–PZT samples. This is because the technique of Ni electrode attachment was newly proposed in recent years.

Several researchers have reported that the poling direction could change the crack growth and material properties of PZT ceramics. Zhao et al. have examined the crack growth characteristics of PZT, and they found that there exists a strong anisotropy of crack growth.[7] In the orientation perpendicular to the polarization direction, cracks grow readily whereas no obvious propagation is found parallel to the polarization direction. Fett et al. have examined the effect of the poling process on the material properties, and it appears that the PZT, poled perpendicular to the external load, shows a stronger plastic deformation than the unpoled material.[8] In the study by Okazaki, the crack extension mechanism in piezoelectric ceramics appeared to be variable because of the internal stress generated by the poling process.[9] His claims were, however, countered by the work

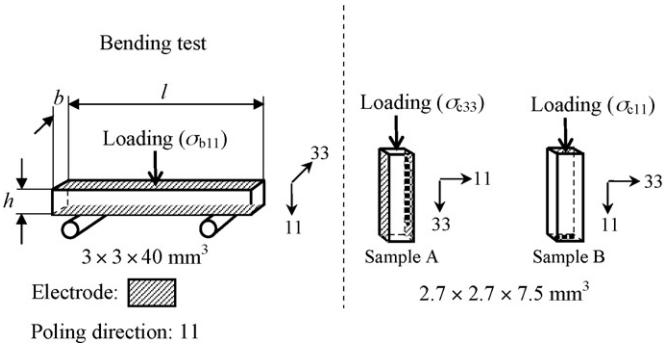

Fig. 1. Specimen samples for bending and compression tests.

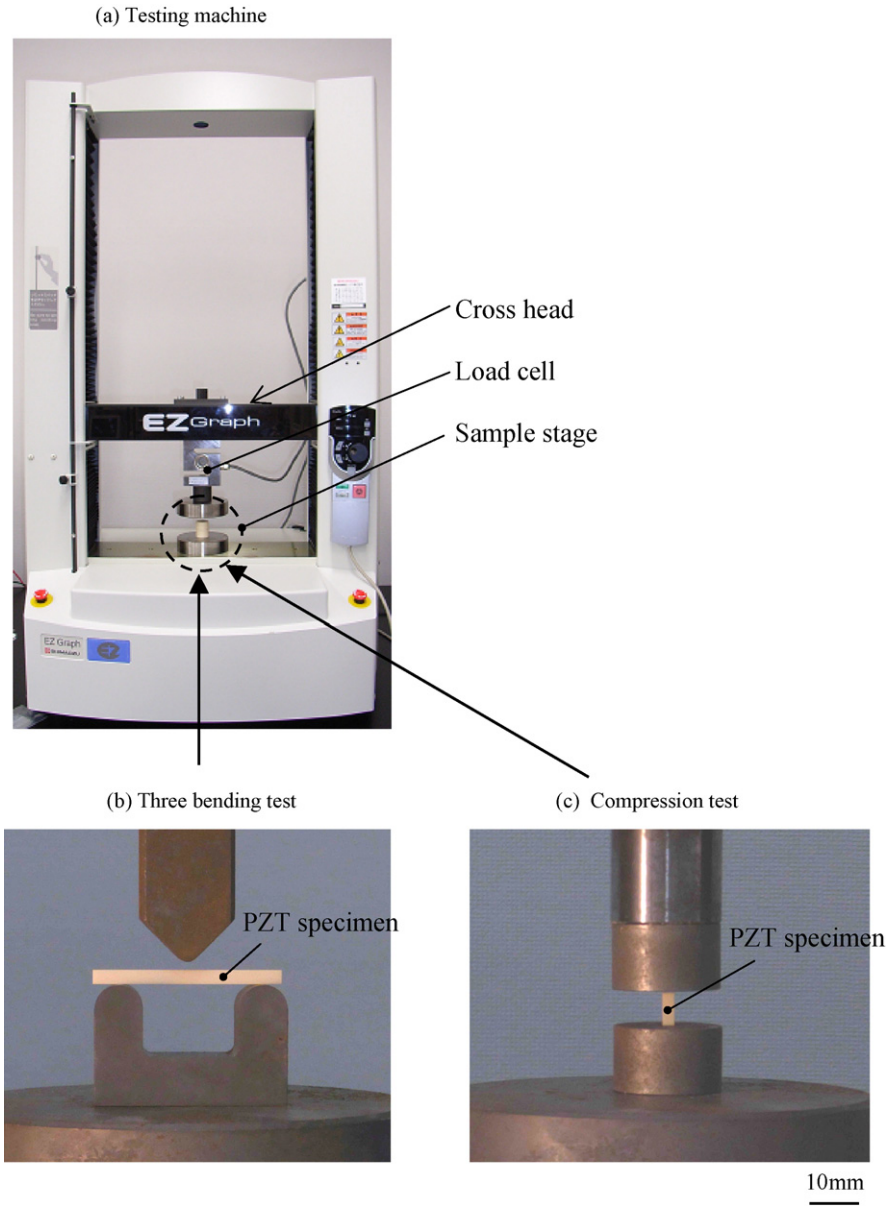

Fig. 2. (a) Screw driven type universal testing machine and (b) and (c) experimental setup for bending test and compression test.

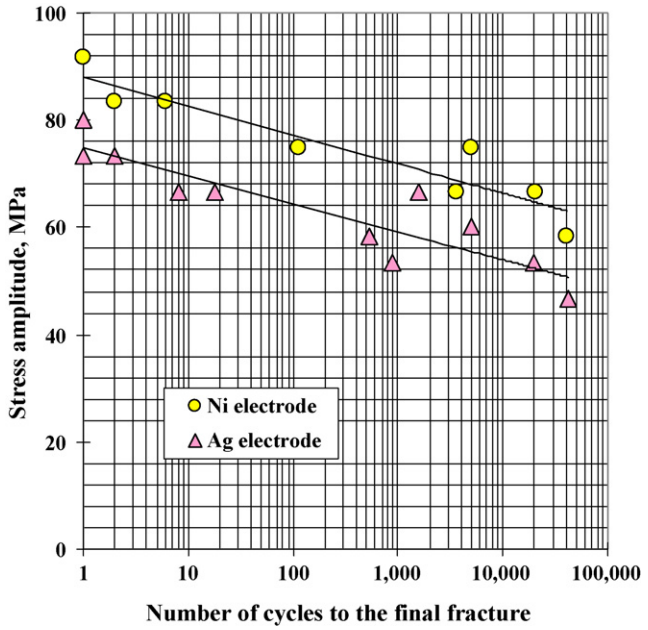

Fig. 3. Stress amplitude vs. cycles to failure in the PZT ceramics with Ni and Ag electrodes.

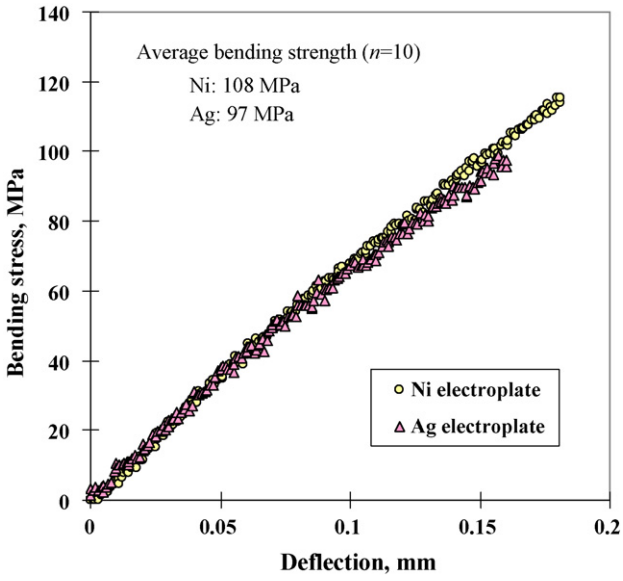

Fig. 4. Relationship between the bending stress and deflection for Ni and Ag samples.

of Mehta and Virkar, since the calculated internal stress in the ceramics was as high as 14.5 GPa, whereas the material hardness of the related ceramics was only 0.47 GPa.[10] Even though the mechanical properties of PZT ceramics could be altered by the electrode and poling direction, the reason for this has not been explained clearly and there is no clear evidence for the explanation. In addition, little work has been done to investigate the failure mechanism and the material properties during the fatigue test. The aim of this work was therefore to examine the fatigue failure characteristics of PZT using samples with (i) different electro plating materials (silver and nickel) and (ii) a different poling direction. Moreover, an attempt was made to interpret clearly the influence of the electrode and polarization on their mechanical properties.

2. Experimental procedures

2.1. Materials

The piezoceramic selected for the present investigation was a commercial bulk lead zirconate titanate ceramic ($PbZrTiO_3$), produced by Fuji Ceramics Co. in Japan. The nominal grain

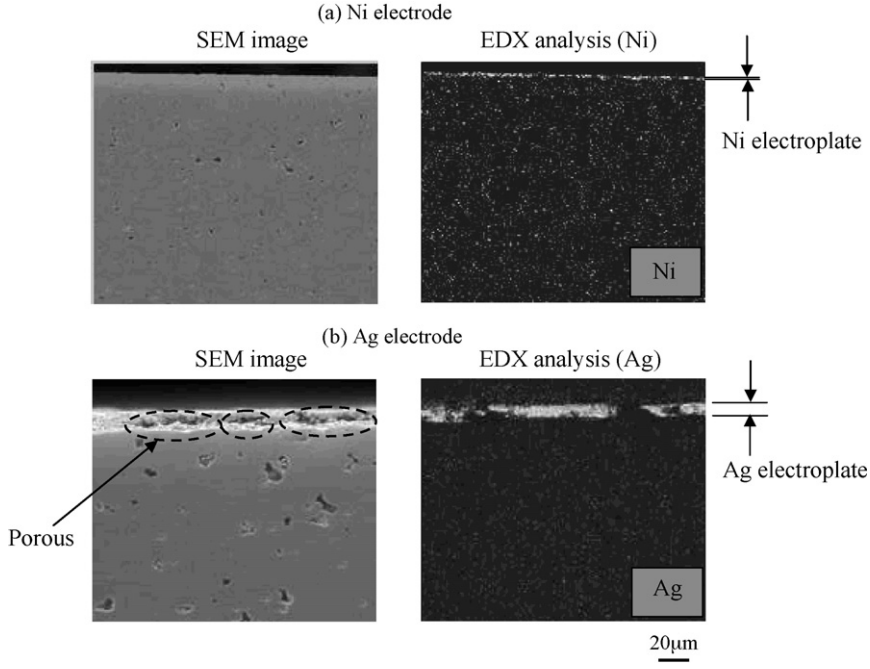

Fig. 5. SEM images and EDX analysis of PZT ceramics near the plating for (a) Ni and (b) Ag.

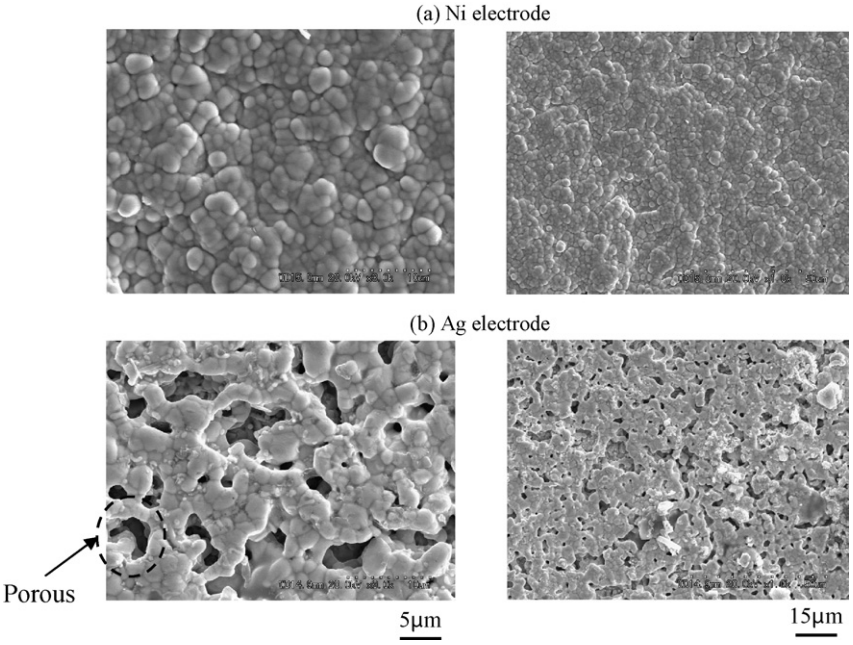

Fig. 6. SEM micrographs showing the surface of the plating: (a) Ni and (b) Ag.

size of this ceramic is approximately 5 μm. The PZT ceramics adopt a tetragonal perovskite structure with $a = b = 0.4046$ nm and $c = 0.4103$ nm at room temperature. The aspect ratio of c/a, examined by X-ray diffraction (XRD), is about 1.014. Two rectangular rod specimens with dimensions 3 mm × 3 mm × 40 mm (for the bending tests) and 2.7 mm × 2.7 mm × 7.5 mm (for the compression tests) were used in the present work (see Fig. 1). In the sample for the compression tests, the electrode was attached in various orientations. Furthermore, two electrode materials were employed, e.g., silver (Ag sample) and nickel (Ni sample). The electrodes were created on the PZT using different processes. The Ag electroplating is printed on the specimen by firing for several hours in atmosphere at 973 K after silver powder is coated on the PZT surfaces. In contrast, the nickel electrode is attached to the PZT surfaces by electroplating in a plating bath. After the electroplating process, the polarization between the two electrodes was conducted. After the electrode attachment, the samples were immersed in silicon oil and electrically poled using electric fields at 2 kV/mm. The material properties of both PZT ceramics (Ag and Ni sample) after polarization, examined by an impedance analyzer (Agilent Technologies, 4294A), are almost same level: the piezoelectric coefficient (d_{33}) for Ag and Ni samples are 472 and 455 pm/V, respectively. Note that the PZT ceramic samples used in the present study were all produced in the same production lot, ensuring similar material quality. In fact, the density of the PZT samples (ρ), measured using Archimedes principle, was almost constant at between 7.56 and 7.59.

2.2. Experiments

The bending and compression tests were performed on the PZT ceramics using a screw driven type universal testing machine with 10 kN capacity. Fig. 2 shows the testing machine and the experimental setup for the bending and compression tests. The resolutions of load and displacement in this testing machine are 0.01 N and 1 μm, respectively. The loading speed for the bending and compression tests was 1 mm/min to the final fracture. The bending fatigue test was also conducted at a frequency of 0.05 Hz and $R = 0.05$. The maximum cyclic load, σ_{max}, was determined on the basis of the bending strength (σ_B), where σ_{max} is designed to be less than 90% of σ_B. The bending stress was calculated using the simple formula $\sigma = 3\Delta Pl/2bh^2$, where P is the applied load, l is the loading span, and h and b are the specimen height and width, respectively. The cyclic loading was applied along the direction of the normal to the electrode surface (see Fig. 1). Note in the fatigue tests a low measurement frequency was employed to reduce the mechanical damage in the sample, and R-ratio of 0.05 was used to make comparison with the related experimental data obtained in our previous works.[11]

2.3. Domain structure

In the present work, an attempt was made to observe the domain structure (crystal orientation and domain wall) by an etching technique with electron back scatter diffraction (EBSD) analysis. The process of the etching technique is as follows: the sample surface for the observation was first polished to a mirror finish using colloidal silica; the sample surfaces were then etched using an etchant consisting of 5 ml hydrochloric acid, 2 ml hydrogen fluoride and 250 ml water. After the etching process, the sample surface was electrically coated, and the surface observation conducted using a scanning electron microscope (SEM).[12,13] The domain structure was also examined by EBSD analysis with an orientation imaging microscopy (OIM)

system. In this approach, the sample is coated with carbon on the polished surface before the analysis. The fundamentals of the EBSD technique are summarized by Randle.[14]

3. Results and discussion

3.1. Fatigue and mechanical strength

Cyclic bending stress was applied to evaluate the fatigue strength and fatigue resistance. The relationship between the stress amplitude and fatigue life, i.e., the S–N diagram, for the PZT ceramic with nickel and silver electrodes is shown in Fig. 3. It is clear that the S–N relationship for the nickel sample is located at a higher level compared to the silver one. The mean endurance limit for the nickel sample at 10^5 cycles is about 60 MPa; this limit is about 1.2 times higher than that for the silver one. Note the S–N curve for Ag obtained is similar to the related data examined in our previous work.[11] In a previous study, it was reported that domain switching in the PZT ceramic could begin when the PZT is loaded with approximately 50 MPa.[10,15] Because the endurance limit of our PZT samples (Fig. 3) is close to the stress level (50 MPa), the fatigue strength of PZT might be related to the domain switching. Details of this will be discussed in a later section of this paper.

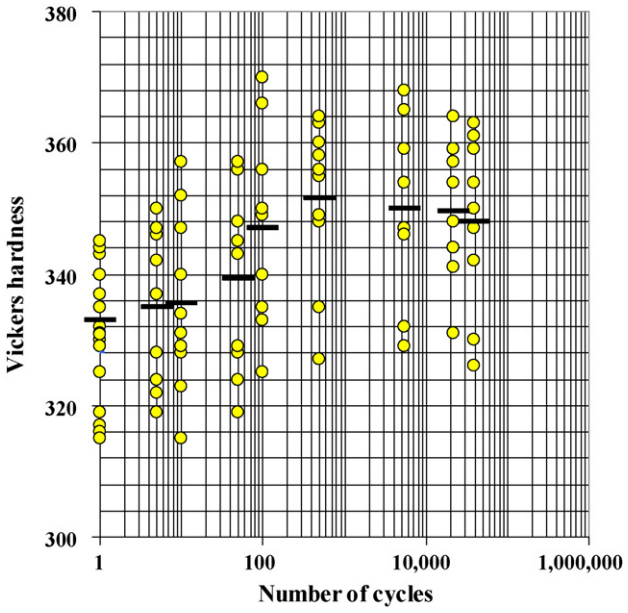

Fig. 8. Variation of the hardness of the PZT ceramics as a function of the cycle number.

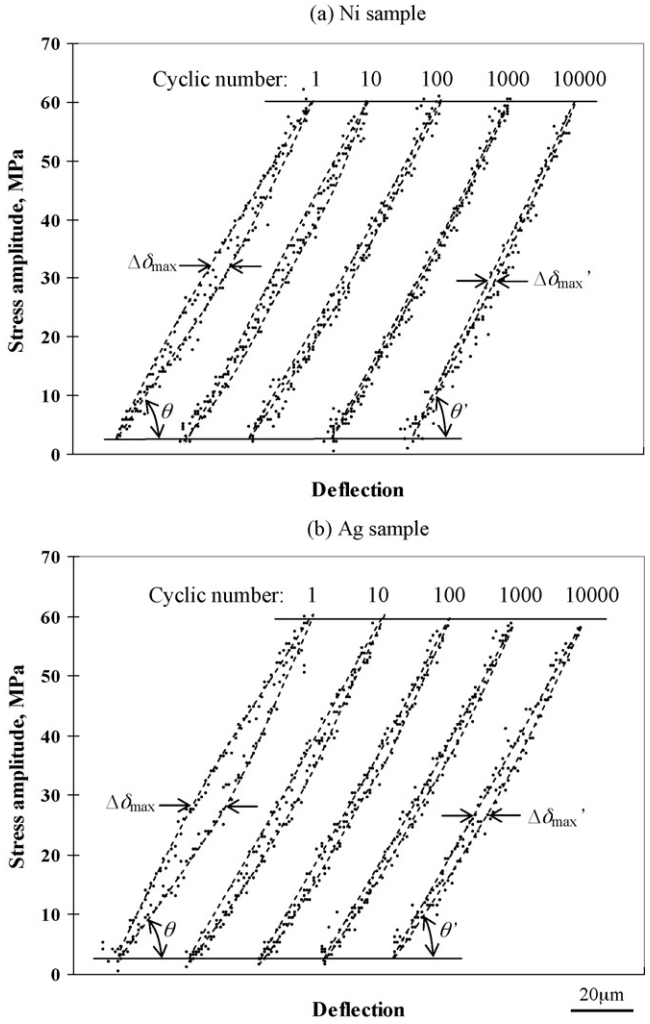

Fig. 7. Stress vs. deflection of PZT ceramics with Ni and Ag electrodes at several stages.

Fig. 4 shows representative bending stress vs. deflection curves for the Ni and Ag samples. The applied load increases linearly with increasing deflection value for both samples until fracture. This result implies that the ceramic has a brittle material property. From Fig. 4, it also appears that the bending strength for the PZT with Ni electroplate is about 10% higher than that for the Ag one; the average bending strengths of Ni– and Ag–PZT are 108 and 97 MPa, respectively. In this case, the different bending strengths may be related with the electrode characteristics attached to the PZT ceramic. To explain this clearly, direct observations of the electrode were conducted. Fig. 5 displays the SEM images and EDX analysis (energy dispersive X-ray spectroscopy) of the cross-section of the PZT adjacent to the Ni- and Ag-electrode. As in Fig. 5, the electroplated thickness is different; the silver electrode is about 10 μm thick, which is about ten times thicker than that of the nickel electrode. In addition, a porous-like zone can be seen in the silver electrode. Fig. 6(a) and (b) represents the SEM images of both plating surfaces. It is obvious that pores are created in the Ag electrode, caused by the high temperature of the firing process for the electrode attachment, as mentioned previously. In contrast, a high density electrode, with small crystallites, is formed with Ni. The SEM observations suggest that the surface roughness of the electrodes would be different. To substantiate this, the surface roughness of both electrodes was examined directly using a surface roughness measuring machine with a resolution of 1 nm. The roughness levels obtained for the Ag and Ni electrodes are $R_a = 0.64$ μm and $R_a = 0.45$ μm, respectively. Such a difference in the surface roughness makes for a different degree of stress concentration. Hence, poorer mechanical properties may have been obtained for the Ag sample (Figs. 3 and 4).

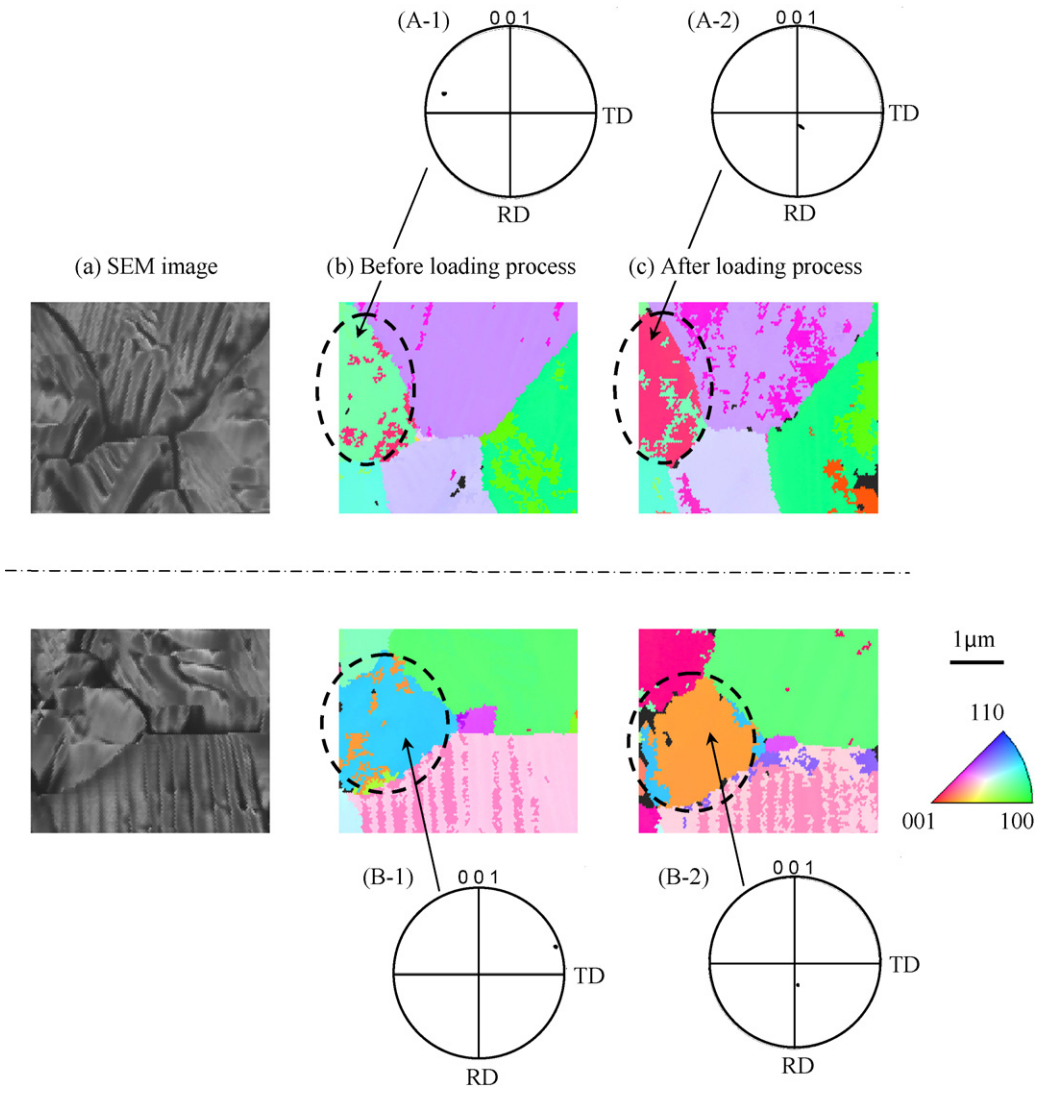

Fig. 9. EBSD analysis of the PZT ceramics after the etching technique: (a) image quality map and (b) and (c) crystal orientation map before and after loading.

3.2. Failure characteristics

The failure characteristics of the PZT ceramic during cyclic loading were investigated. Fig. 7 shows the stress–deflection curves over several cycles for the Ni and Ag samples. It should be pointed out first that the deflection value in this sample was evaluated directly with the displacement level of this testing machine. The reasons behind this are that (i) the testing machine has high resolutions (1 μm) as mentioned previously and (ii) the specimen stiffness is lower than that for the test fixtures, e.g., Young's modulus of the PZT specimen (52 GPa[16]) is quarter of the testing fixtures (hardened steel = 206 GPa). Furthermore, this approach was carried out with several samples to verify the experimental data. As can be seen, a hysteresis loop of load vs. deflection relationship is obtained in both samples although the loop profile is different. With increasing cycle number (i) the deflection value between the loading and unloading phases ($\Delta\delta_{max}$) decreases and (ii) the slope of load vs. deflection (θ) increases. It is also clear that the $\Delta\delta_{max}$ level for the Ag sample (Fig. 7(b)), especially in the first cycle, is greater than that for the Ni sample (Fig. 7(a)). This would be associated with the different electrode properties, as described previously. It should be descried that the decrease of $\Delta\delta_{max}$ during the fatigue test has a different trend to that for an annealed medium carbon steel. In carbon steel, $\Delta\delta_{max}$ increases due to softening of the material.[17] Based upon this, it might be that the PZT ceramic is being hardened during the cyclic loading. Fig. 8 displays the variation of the Vickers hardness of the PZT as a function of cycle number. Note in this approach the fatigue test was carried out at $\sigma_{max} = 50$ MPa and the hardness measurement was executed in the sample in the high tensile stress region. Although the hardness data is widely scattered, the material hardness seems to increase with increasing number of cycle. In this case, the material hardening may be influenced by domain switching.[17,18] Several researchers have reported that domain switching could change the material properties.[19,20]

To clarify whether or not domain switching occurs in our PZT ceramics, the crystal structure orientation before and after loading was investigated in the same area. In this case, a compressive load was conducted in a localized area of the sample

surface (1 cm^2) with a load of 5 kgf adjacent to the observation region. Fig. 9(a) displays the SEM image of the PZT and Fig. 9(b) and (c) presents the crystal orientation maps (EBSD) before and after loading. The color level of each pixel in the crystal orientation map is defined according to the deviation of the measured orientation with respect to the ND direction (see the color key of the stereographic projection). As seen in the SEM micrograph Fig. 9(a), a rough sample surface (shaped like a groove) is observed due to the etching process. In this case, such a groove could be related to the domain boundary. From the EBSD analysis, the crystal orientation in the grain is different depending on the grain (see Fig. 9(b)). It is clear that, after the loading process, the crystal orientation in some grains changes from domain to domain by 90°, i.e., domain switching. For instance, the domain orientation in the area, pointed by the arrow (the green color zone, A-1), is (2 1 0) before loading, but is tilted to (1 0 2) in the red color zone (A-2) following the loading process. This result infers that domain switching can occurs anywhere in the grains, which makes for a high internal stress, leading to material hardening of the PZT, as shown in Figs. 7 and 8. A similar approach was carried out in the study by Kimachi et al.,[12] where the domain switching characteristics around the cracks were observed by EBSD analysis.

3.3. Domain structures

To examine the effect of domain structure on the mechanical properties of the PZT ceramic, static compression tests were carried out using the Ag-PZT sample with a different poling direction, e.g., (i) σ_{c33}: stress direction ⊥ poling direction; (ii) σ_{c11}: stress direction//poling direction. The results obtained are shown in Fig. 10. It is clear that the compression strength for σ_{c11} is higher than that for σ_{c33}. This result indicates that the material strength of the PZT is attributed to the loading direction and poling direction. Fett et al. and Ende et al. investigated the effects of the poling process on the deformation characteristics in PZT.[21,22] One of their conclusions was that the stiffness of PZT could be low whilst the poling process is conducted. To explain the relationship between the poling direction and the mechanical properties, the microstructural characteristics of the PZT ceramic were investigated. Fig. 11 presents the SEM images for the PZTs after etching: (a) without poling and (b)–(d) with the poling process. Note that the poling direction is different in the sample between Fig. 11(b) and (c). The micrograph in Fig. 11(d) is the three point bending specimen fractured by the fatigue test. As seen in Fig. 11(b)–(d), a typical etch pattern can be seen, where the groove shape (domain wall) is revealed in the grain, even though no clear domain wall is detected in the unpoled one (Fig. 11(a)). Because the groove formation is only seen in the poled samples, this must be related to the poling process. It is interesting to note that the domain wall is ideally aligned in the grain perpendicular (orthogonal) to the poling direction, (see Fig. 11(b) and (c)).[13] Fig. 12 shows the angle of the domain wall direction, θ, measured from a hundred grains. It is obvious that a number of domain walls are directed perpendicular to the poling direction, i.e., 75% of the domain walls are formed between 70°

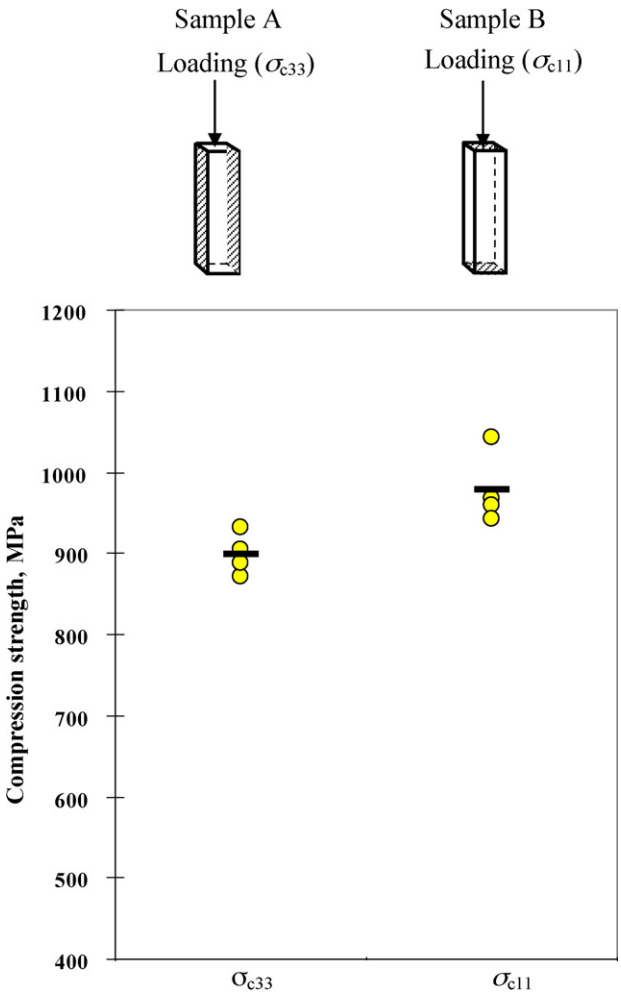

Fig. 10. Compression strength for the samples with different poling directions.

and 110°. In the study by Hatanaka and Hasegawa, they pointed out that the grooves remain stable as the inhomogeneous stress is applied to the PZT[23]; the direction of the groove might be related to the <1 0 0> direction and the deeply etched area associated with the a-face. Anteboth et al. also observed the domain direction in the PZT ceramic using a scanning force microscope and detected different domain orientations.[24] Although several investigators have observed domain wall formation in PZT grains, there is no clear explanation for the relationship between the poling direction and the domain wall orientation. The creation of an aligned domain wall might be a result of: (i) an electric dipole moment and (ii) a high applied stress. An applied electric field could change the relative displacement of the positive and negative ions, which induces the deformation of the crystal structures.[25] Also, a high applied stress might make the domain wall move (see Fig. 13). A similar model was reported by Gruverman et al.[26]. They mentioned that the applied electric field might result in a 90° rotation of the polarization vector, so that a 90° domain wall could be created.

The crystal orientation in the domain wall was further examined using the fractured sample. Fig. 14(a) and (b) displays the SEM image and the crystal orientation map and Fig. 14(c) shows the pole figures, measured with orientations (0 0 1), (1 0 0) and

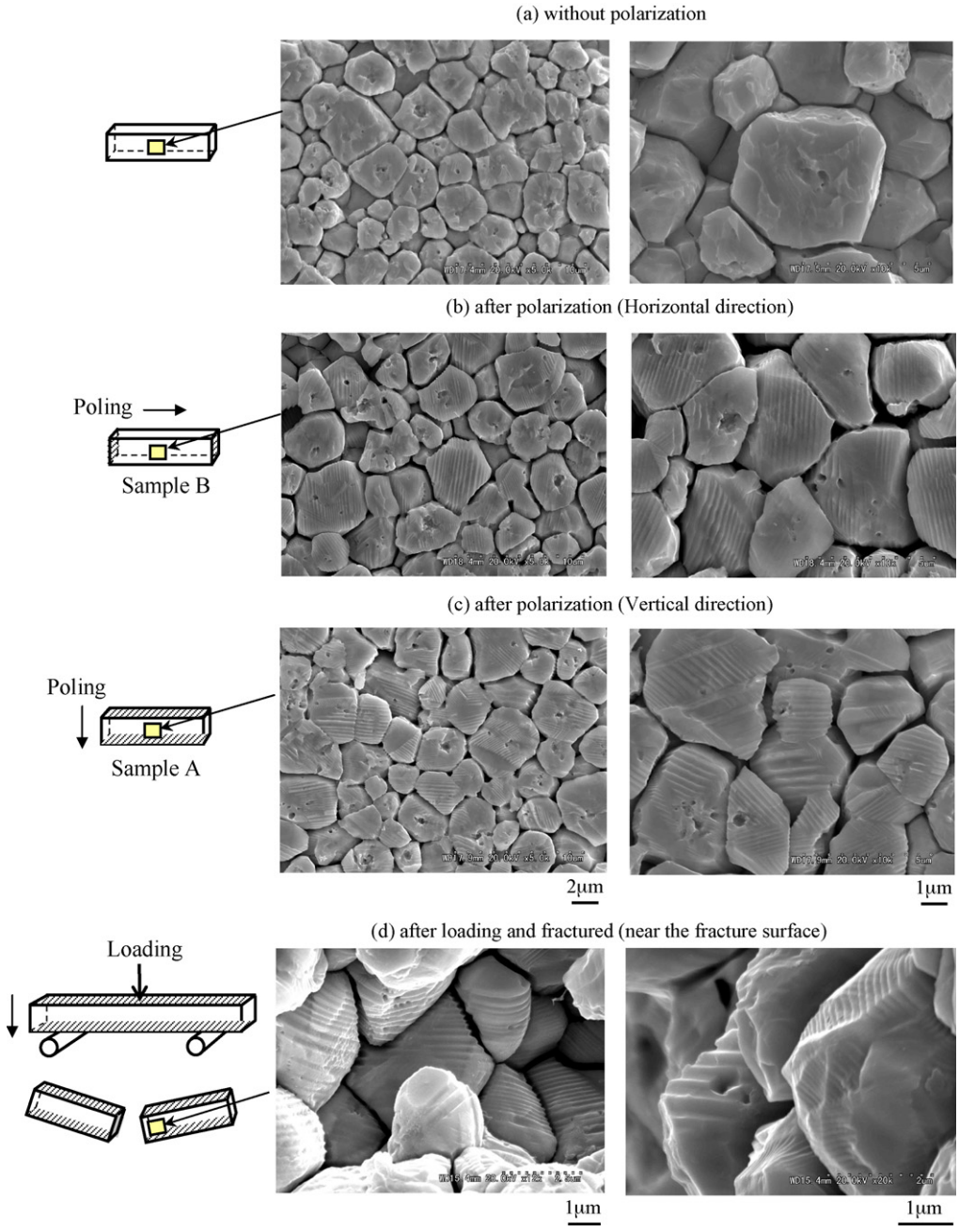

Fig. 11. Microstructures of the PZT ceramics after the etching technique: (a) sample without poling; (b) and (c) after poling and (d) after loading and fracturing.

(1 1 0), derived from the EBSD crystallographic map. Different crystal plane orientations in the grain can be seen, indicated by different colors. Such a random structural orientation is observed clearly in the pole figures. The (1 0 0) and (1 1 0) pole figures exhibit some agreement with those for the associated PZT examined in the work by Tai et al.[27]. It is also observed that some crystal orientations in the area of the deeply and lightly etched zones are altered, e.g., the domain orientation in the deeply etched zone (2 0 1) and (1 0 5), and the lightly etched zone (2 1 0) and (5 1 0), as enclosed by the dashed circles. The angle of the misorientaion between the two zones was further investigated, and the results are displayed in Fig. 15. Fig. 15(a) features a grain map showing the misorientation zone with the angle between 85° and 90°. In this case, the assessment was done individually with every grain. From this grain map, the deeply etched zone seems to be tilted by about 90°. It is further clarified from Fig. 15(b) that a large number of the domains in the deeply etched area are tilted between 85° and 90°. This result is in good agreement with the data examined by Kimachi et al.[12]. On the basis of the this EBSD analysis, the domain orientation of the PZT can be schematically illustrated in Fig. 16, showing the different domain direction (90°) and the aligned domain wall. Such an anisotropic structure could reflect the mechanical strength of the PZT. Several researchers have reported that anisotropic crystal orientation results in (i) high internal and external stresses, (ii) nonsymmetrical defor-

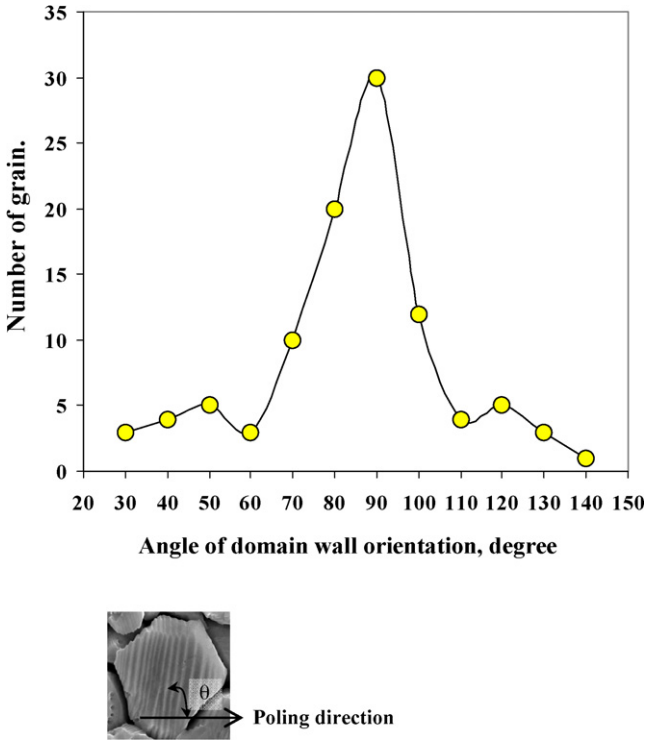

Fig. 12. Angle of the domain wall orientation on the basis of the poling direction ($n = 100$).

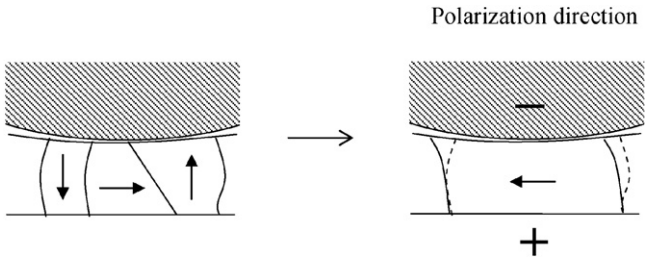

Fig. 13. Diagram illustrating 90° rotation of the domain wall motion in the grain due to a high compressive stress exerted by the poling process.

mation and (iii) nonlinear material hardening during tension and compression loading.[1,8,28]

3.4. Crack growth characteristic

The effect of the domain orientation on the crack growth characteristic was investigated by the indentation tests. In this test, a Vickers diamond indenter with a sufficient load, e.g. 9.8 N, introduces surface cracks from the corners of the indents. The diamond pyramid indenter was selected because of its general facility for reproducing well-defined radial crack traces on ceramic surfaces. Samples with different poling directions were employed in this test. Fig. 17 depicts the cracks in the PZT samples. As seen, the crack propagates readily when it grows along the groove direction, while the crack length is found to be short in the direction perpendicular to the groove. The average

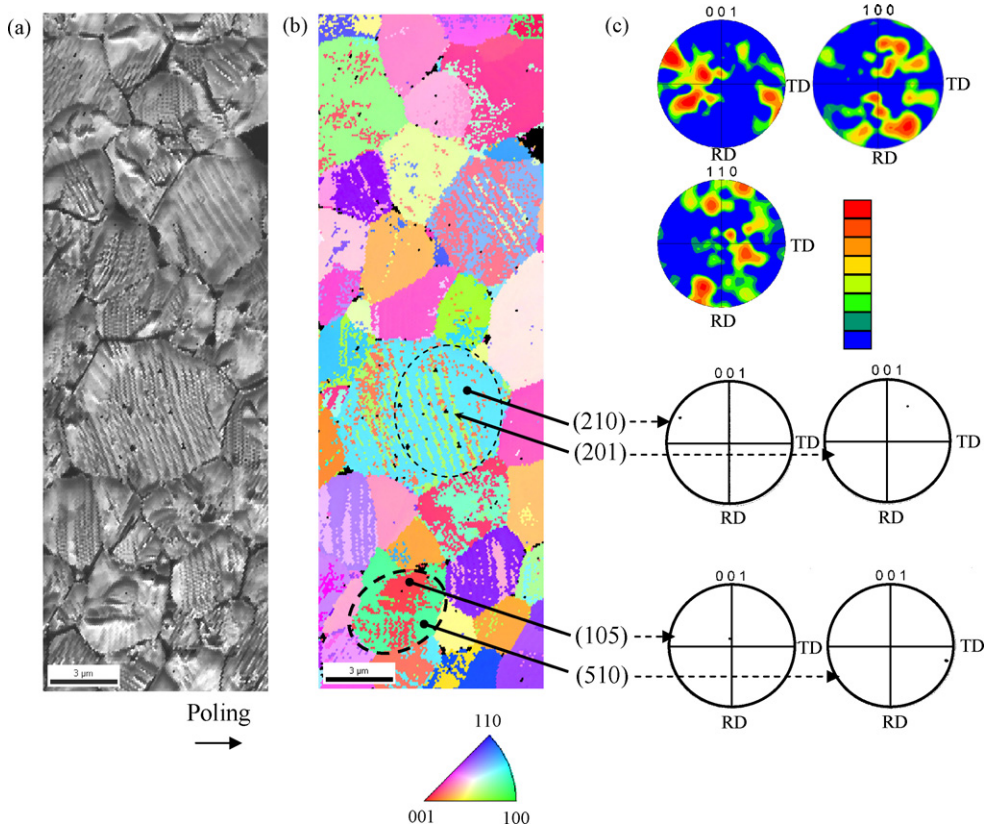

Fig. 14. EBSD analysis of the PZT ceramics after the etching technique: (a) image quality map and (b) crystal orientation map and (c) the (0 0 1), (1 0 0) and (1 1 0) pole figures.

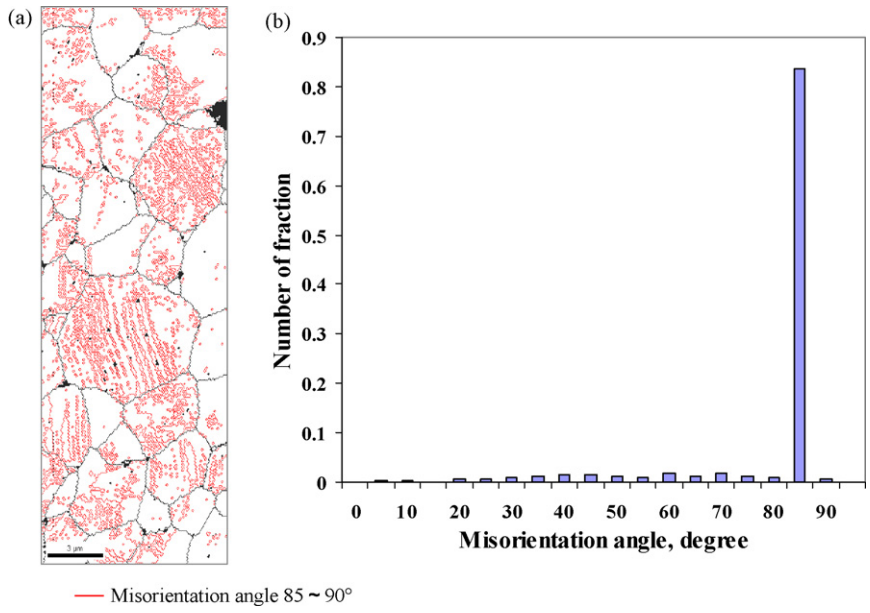

Fig. 15. (a) Grain map showing misorientaion zone with the angle between 85° and 90°; (b) misorientation angle chart.

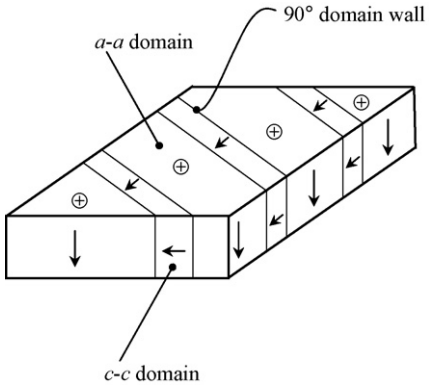

Fig. 16. Schematic illustration showing the domain direction of the PZT grain.

Table 1
The average crack length for a_{11} and a_{33}.

	a_{33}	a_{11}
Sample A	1.79 (long)	1
Sample B	1.82 (long)	1

The length is expressed as a ratio based on the short crack length.

crack length ($n = 25$) is shown in Table 1, relative to the average of the short crack lengths. There exists a strong anisotropic crack growth characteristic. The crack length perpendicular to the poling direction a_{33} (⊥ poling) is about twice as great as that parallel to the poling direction a_{11} (//poling). Such a significant anisotropy in crack growth is dependent on the domain characteristics. Fig. 18 shows the SEM images of the crack growth

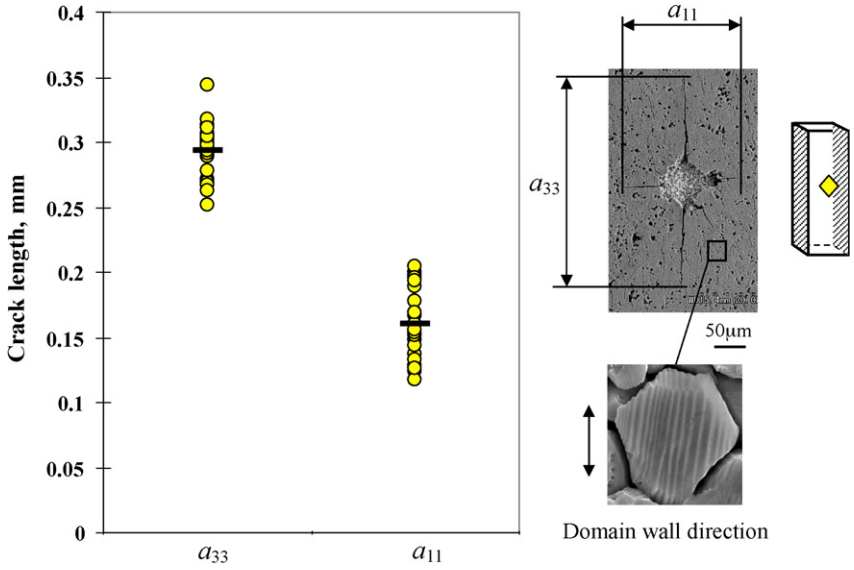

Fig. 17. Crack length obtained by the Vickers indentation for Sample A.

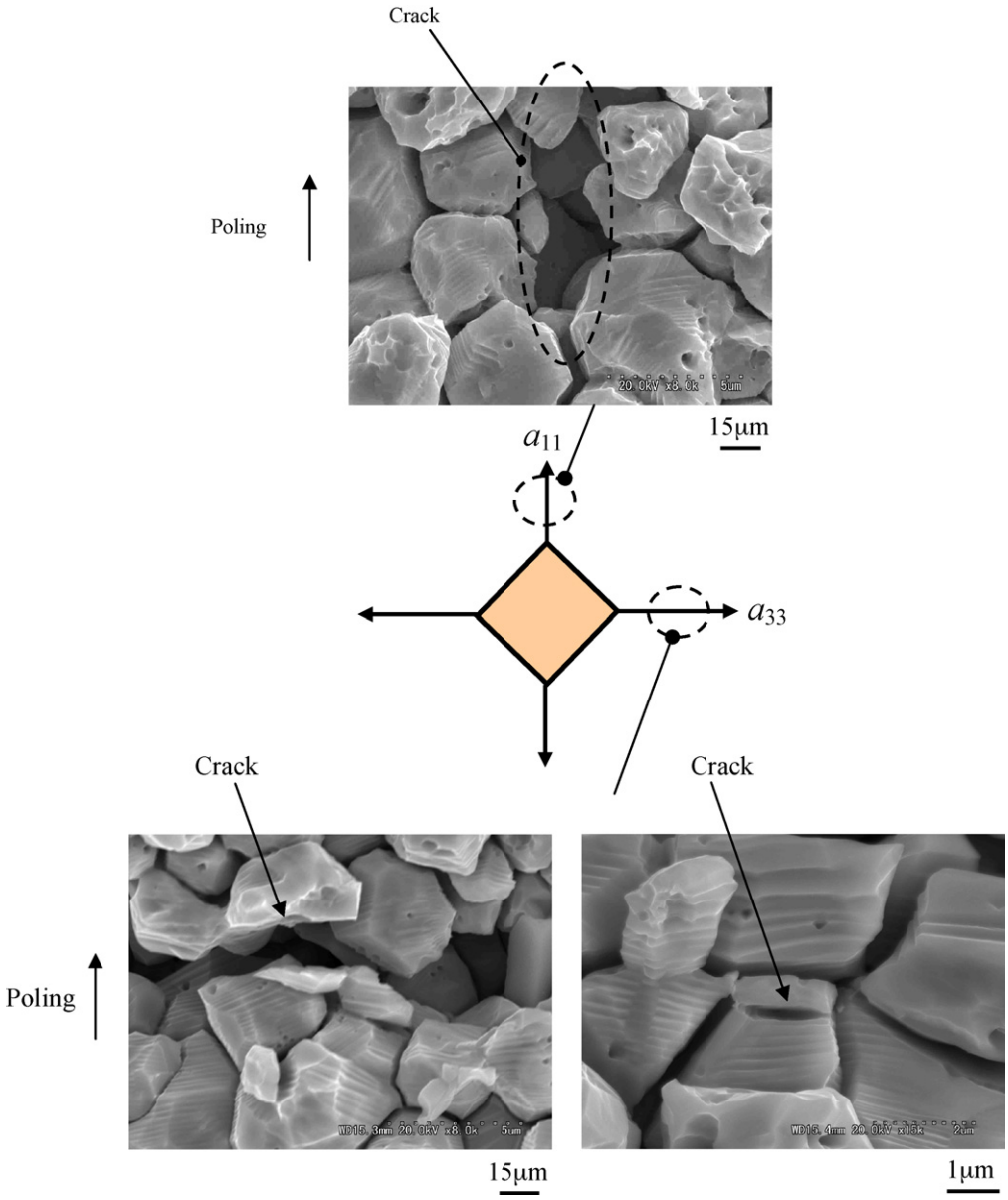

Fig. 18. SEM micrographs showing the indent crack.

characteristics in the PZT around the indentation. It is clear that the crack follows a well-defined fracture path along the domain boundary. This accelerates the crack growth (a_{33}), leading to low fracture toughness. In contrast, the crack propagates along the grain boundary for a_{11}, which gives high crack growth resistance. This result suggests that the groove formation in the grain is attributed to the failure characteristics and the mechanical properties. Similar crack growth characteristics have also been obtained by other researchers. Cheng et al.[29] examined the effect of poling direction on the crack growth characteristic in the PZT, and the crack is sharp in the sample poled perpendicular to the notch, i.e., a_{33}. In contrast, the crack surface is significantly damaged in the sample poled parallel to the notch, i.e., a_{11}s[9,29] Several investigators have suggested that the different crack growth characteristics are influenced by the residual stress[9] and domain switching. Zhao et al. pointed out that the different crack growth length is influenced by the domain switching.[7] Furthermore, Tobin and Pak reported that domain wall switching, occurring at the crack tip parallel to the poling direction, is responsible for absorbing the fracture energy, hence giving an apparent increase in fracture toughness in that direction.[30] Although no clear explanation is reported in their work, the different crack growth characteristic could also be related to the groove formation in the grains. Also confirmed is the importance of estimating the fracture toughness of our PZT ceramics. The fracture toughness of K_{IC} can be estimated using the following equation[30,31]:

$$K_{IC} = 0.0113 \frac{d}{a^{3/2}} \sqrt{FY} \quad (1)$$

where d is the diagonal length of the indented pyramid base, a is the crack length, F is the applied indentation force and Y

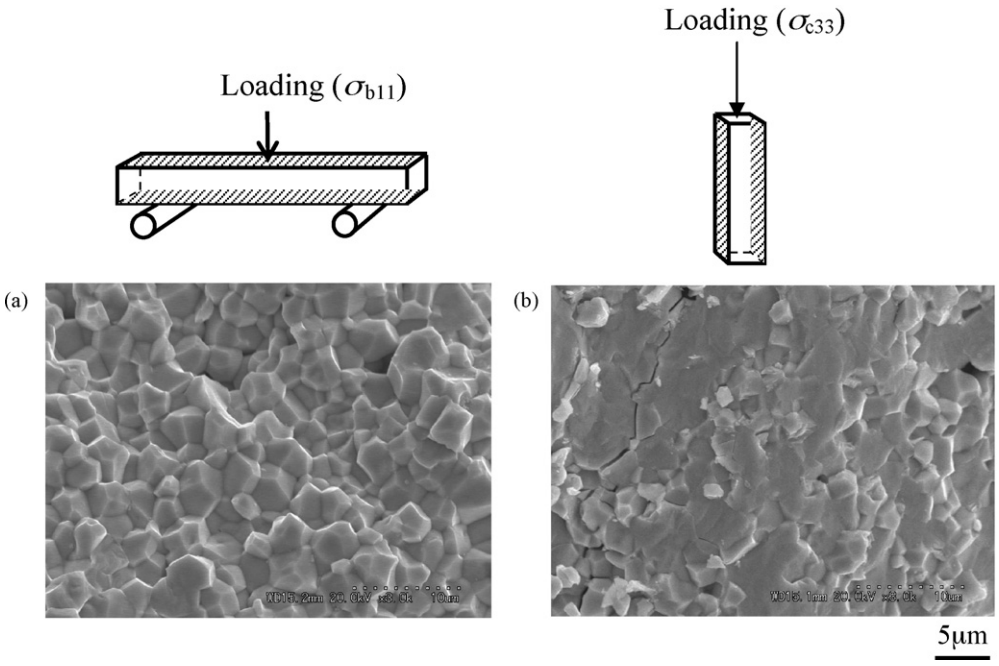

Fig. 19. SEM micrographs of the fracture surfaces after (a) bending test and (b) compression test.

is the Young's modulus of the ceramic. The average diagonal indentation is 60 μm. The Young's modulus of the PZT ceramic is $Y_{11} = 58$ and $Y_{33} = 52$ GPa.[16] The average crack lengths of a_{11} and a_{33} obtained in Fig. 17 are 161 and 293 μm, respectively. From Eq. (1), the calculated fracture toughness values $K_{IC,11}$ and $K_{IC,33}$ are 0.237 and 0.102 MPa$\sqrt{}$m, respectively. The fracture toughness $K_{IC,11}$ is about 2.3 times higher than $K_{IC,33}$, and this result is close to that for similar PZT ceramics examined by other researchers.[31] This approach (Fig. 18) shows that fracture characteristics in the PZT can be changed, depending on domain orientation. Fig. 19(a) and (b) displays the SEM images of the fracture surfaces for the samples after bending and compression tests (σ_{b11} and σ_{c33} directions). As can be seen, an intergranular based fracture is obtained for the σ_{b11} sample, whereas a mixture of transgranular and intergranular fractures is the dominant feature for σ_{c33}. Such a change of the fracture characteristic would also be affected by the crack growth characteristic in Fig. 18.

4. Conclusions

Fatigue failure characteristics of the lead zirconate titanate piezoelectric ceramics have been studied experimentally. In this experiment, PZT ceramics having different electrode materials and different poling directions were employed. Based upon the above results and discussion, the following conclusions can be drawn.

(1) The fatigue strength for the nickel sample is about 1.2 times higher than that for silver sample. The bending strength for the Ni sample is about 1.1 times higher than the Ag sample. The different mechanical strengths are attributed to the characteristics of the electroplating on the PZT ceramic. A porous layer is created in the Ag electrode, while a high density layer with a smooth face is formed with the Ni electrode. The surface roughness for the Ag electrode is approximately 1.2 times higher than for the Ni electrode and this could lead to different mechanical properties.

(2) The deflection value of the PZT ceramics decreases with increasing cycle number. The change of the deflection is attributed to the material hardness. The material hardening occurs due to the domain switching, which is clearly detected via the EBSD analysis. The domain wall orientation shows the grooves in grains, and the domain wall direction is formed perpendicular to the poling direction.

(3) The mechanical properties of PZT are directly influenced by the domain wall orientation; crack propagation occurs mainly along the domain wall boundary for a_{33}, whereas the crack propagates in the grain boundary for a_{11}. The fracture toughness $K_{IC,11}$ is about 2.3 times higher than $K_{IC,33}$ due to the different crack growth resistance. The crack growth characteristic produces a different fracture pattern, with intergranular based fractures in the PZT when loaded with σ_{11} and a mixture of transgranular and intergranular fractures when loaded with σ_{33}.

Acknowledgements

This work was financially supported by a research granted from the Murata Science Foundation in Japan. The authors would like to express the appreciation to Mr. H. Tojo at TDK Corporation for helpful comments and suggestions on the manuscript. The authors would also appreciate Mr. K. Funatsu at Foundation for Promotion of Material Science and Technology of Japan for his technical support.

References

1. Huang, H. and Hing, P., Energy balance model for the Vickers hardness of ferroelectric PZT ceramics. *J. Mater. Sci. Lett.*, 1999, **18**, 1675–1677.
2. Oates, W. S., Lynch, C. S., Lupascu, D. C., Njiwa, A. B. K., Aulbach, E. and Rödel, J., Subcritical crack growth in lead zirconate titanate. *J. Am. Ceram. Soc.*, 2004, **87**, 1362–1364.
3. Guillon, O., Thiebaud, F. and Perreux, D., Tensile fracture of soft and hard PZT. *Int. J. Fracture*, 2002, **117**, 235–246.
4. Koo, J. M., Bang, I., Kim, T., Lee, J. G. and Kim, J., Effects of hybrid structure top electrodes of PZT capacitors on hydrogen-induced damage. *J. Korean Phys. Soc.*, 2001, **38**, 273–276.
5. Okayasu, M., Aoki, S. and Mizuno, M., Effects of silver-based metal electroplate on fatigue properties of PZT ceramics. *Int. J. Fatigue*, 2008, **30**, 1115–1124.
6. Zhang, T. Y., Effects of static electric field on the fracture behavior of piezoelectric ceramics. *Acta Mech. Sin.*, 2002, **18**, 537–550.
7. Zhao, J., Yue, Z., Wang, W., Gui, Z. and Li, L., Characterizations of fatigue and crack growth of ferroelectrics under cyclic electric field. *J. Electroceram.*, 2008, **21**, 581–584.
8. Fett, T., Müller, S., Munz, D. and Thun, G., Nonsymmetry in the deformation behaviour of PZT. *J. Mater. Sci. Lett.*, 1998, **17**, 261–265.
9. Okazaki, K., Mechanical behavior of ferroelectric ceramics. *Bull. Am. Ceram. Soc.*, 1984, **63**, 1150–1152.
10. Mehta, K. and Virkar, A. V., Fracture mechanisms in ferroelectric–ferroelastic lead zirconate titanate [Zr:Ti = 0.54:0.46] ceramics. *J. Am. Ceram Soc.*, 1990, **73**, 567–574.
11. Okayasu, M., Otake, M., Bitoh, T. and Mizuno, M., Temperature dependence of the fatigue and mechanical properties of lead zirconate titanate piezoelectric ceramics. *Int. J. Fatigue*, 2009, **31**, 1254–1261.
12. Kimachi, H., Tsunekawa, T., Shirakihara, K. and Tanaka, K., Observation of crystal orientation, domain and domain switching in ferroelectric ceramics by EBSP method. *J. Jpn. Foundry Eng. Soc.*, 2008, **74**, 335–341 [in Japanese].
13. Fang, F., Yang, W. and Zhu, T., Crack tip 90° domain switching in tetragonal lanthanum-modified lead zirconate titanate under an electric field. *J. Mater. Res.*, 1999, **14**, 2940–2944.
14. Randle, V., *Microtexture Determination and its Applications* (*2nd ed.*). Money, London, 2003.
15. Okayasu, M., Odagiri, N. and Mizuno, M., Damage characteristics of lead zirconate titanate piezoelectric ceramic during cyclic loading. *Int. J. Fatigue*, 2009, **31**, 1434–1441.
16. Fuji Ceramics Co., *Technical Handbook*. Fuji Ceramics Co., p. 36.
17. Okayasu, M. and Wang, Z., Experimental investigation of the effects of artificial wedges on fatigue crack growth and crack closing behavior in annealed SAE1045 steel. *Int. J. Fatigue*, 2007, **29**, 962–976.
18. Hizebry, A., Attaoui, H. E., Saâdaoui, M., Chevalier, J. and Fantozzi, G., Effect of Nb and K doping on the crack propagation behaviour of lead zirconate titanate ceramics. *J. Eur. Ceram. Soc.*, 2007, **27**, 557–560.
19. Pojprapai(Imlao), S., Jones, J. L., Studer, A. J., Russell, J., Valanoor, N. and Hoffman, M., Ferroelastic domain switching fatigue in lead zirconate titanate ceramics. *Acta Mater.*, 2008, **56**, 1577–1587.
20. Jones, J. L., Hoffman, M. and Vogel, S. C., Ferroelastic domain switching in lead zirconate titanate measured by in situ neutron diffraction. *Mech. Mater.*, 2007, **39**, 283–290.
21. Fett, T., Munz, D. and Thun, G., Dielectric parameters of a soft PZT under mechanical loading. *J. Mater. Sci. Lett.*, 2002, **21**, 849–852.
22. Ende, D. A., Bos, B. and Groen, W. A., Non-linear electromechanical behaviour of piezoelectric bimorph actuators: influence on performance and lifetime. *J. Electroceram.*, 2009, **22**, 185–191.
23. Hatanaka, T. and Hasegawa, H., Observation of domain structures in tetragonal $Pb(Zr_xTi_{1-x})O_3$ single crystals by chemical etching method. *Jpn. J. Appl. Phys.*, 1992, **31**, 3245–3248.
24. Anteboth, S., Brückner-Foit, A., Hoffmann, M. J., Sutter, U., Schimmel, Th. and Müller, M., Electromechanical behaviour of PZT with real domain structure. *Comput. Mater. Sci.*, 2008, **41**, 420–429.
25. Fang, D. and Li, C., Nonlinear electric-mechanical behavior of a soft PZT-51 ferroelectric ceramic. *J. Mater. Sci.*, 1999, **34**, 4001–4010.
26. Gruverman, A., Kholkin, A., Kingon, A. and Tokumoto, H., Asymmetric nanoscale switching in ferroelectric thin films by scanning force microscopy. *Appl. Phys. Lett.*, 2001, **78**, 2751–2753.
27. Tai, C. W., Baba-kishi, K. Z. and Wong, K. H., Microtexture characterization of PZT ceramics and thin films by electron microscopy. *Micron*, 2002, **33**, 581–586.
28. Tai, W. P. and Kim, S. H., The effect of poling treatment and crystal structure of PZT on fracture toughness and fatigue resistance. *J. Mater. Sci.*, 2003, **38**, 1787–1792.
29. Cheng, B. L., Reece, M. J., Guiu, F. and Algueró, M., Fractrure of PZT piezoelectric ceramics under compression–compression loading. *Scr. Mater.*, 2000, **42**, 353–357.
30. Tobin, A. G. and Pak, Y. E., Effect of electric fields on fracture behavior of PZT ceramics. *Proc. SPIE Int. Soc. Opt. Eng.*, 1993, **1916**, 78–86.
31. Yang, W., Fang, F. and Tao, M., Critical role of domain switching on the fracture toughness of poled ferroelectrics. *Int. J. Solid Struct.*, 2001, **38**, 2203–2211.